 Communications in Theoretical Physics

Commun. Theor. Phys. **77** (2025) 035301 (10pp) https://doi.org/10.1088/1572-9494/ad7e96

Influence of polarization of hot nuclear matter on the anomaly of surface diffuseness of inter-nuclear potential

S Ramezani Sani[1], R Gharaei[1,2,*] and H A Rahnamaye Aliabad[1]

[1] Department of Physics, Sciences Faculty, Hakim Sabzevari University, PO Box 397, Sabzevar, Iran
[2] Department of Physics, Faculty of Science, Ferdowsi University of Mashhad, PO Box 91775-1436, Mashhad, Iran

E-mail: r.gharaei@hsu.ac.ir and rezagharaei@um.ac.ir

Received 1 May 2024, revised 28 August 2024
Accepted for publication 24 September 2024
Published 6 December 2024

Abstract

The fusion excitation functions for 12 colliding systems with $96 \leqslant Z_1Z_2 \leqslant 608$ are analyzed using coupled-channel (CC) calculations based on the M3Y double-folding (DF) potential supplemented with a repulsive potential that takes into account the incompressibility of the nuclear matter. We also applied the polarization effects of hot nuclear matter (PEHNM) on the calculations of the bare nucleus—nucleus interaction potential within the framework of the modified density-dependent Seyler–Blanchard (SB) approach in the T^2 approximation. Our results reveal that we obtain a nice description of the experimental data of different fusion systems when we use the present theoretical approach to calculate the energy-dependent values of the fusion cross sections. In this paper, the influence of the PEHNM on the surface diffuseness parameter of the Woods–Saxon (WS) potential is also studied. In order to reach this goal, we extract the corresponding values of this parameter based on the modified form of the DF potential (M3Y+Repulsion+polarization). We find that the extracted values are located in a range between $a = 0.61$ and 0.80 fm at different incident energies. It seems that the polarization effects of hot nuclear matter play a key role in describing the abnormally large values of the nuclear potential diffusenesses in the heavy-ion fusion reactions. Additionally, the regular decreasing trend for the diffuseness parameter of the nucleus–nucleus potential with the increase in the bombarding energies is also observed.

Keywords: Heavy-ion fusion reactions, Seyler–Blanchard approach, diffuseness parameter, polarization effects

(Some figures may appear in colour only in the online journal)

1. Introduction

The interaction potential between the projectile and target plays an essential role in the study of heavy-ion fusion reactions. It is well known that this potential consists of the long-range Coulomb repulsion force and the short-range attractive nuclear interaction. The Coulomb component of the inter-nuclear potential can be calculated with great accuracy, whereas the nuclear potential between two colliding nuclei is not yet fully understood. During recent decades, many theoretical approches have been proposed to determine the nucleus–nucleus potential [1–8]. Among various models for nuclear potential, the Woods–Saxon (WS) potential is widely used for analyzing the heavy-ion fusion reactions [9–11] as well as elastic scattering data [12, 13]. Theoretically, the phenomenological WS potential can be parameterized as the following form

$$V_N^{\mathrm{WS}}(r) = -\frac{V_0}{1 + \exp[(r - R_0)/a]}. \tag{1}$$

Here, r refers to the center-of-mass distance between the projectile nucleus with mass number A_{P} and the target nucleus

[*] Author to whom any correspondence should be addressed.

with mass number A_T. Equation (1) reveals that the WS potential is identified with three parameters: the depth V_0, the radius $R_0[=r_0(A_T^{1/3}+A_P^{1/3})]$ and the diffuseness a of the nuclear potential. We note that the diffuseness parameter specifies the potential slope in the tail region of the Coulomb barrier. Therefore, obtaining the quantitative measure for this parameter is of crucial importance. As a result of the literature [14, 15], the surface diffuseness parameter around $a = 0.63$ fm is required to fit adequately the elastic scattering data. Whereas, the extracted values from the sub-barrier fusion data lie within the range $a = 0.75$ to 1.5 fm [16–20]. In this situation, it can be said that the surface diffuseness anomaly in heavy-ion potentials is one of the challenging open problems which has attracted a lot of attention in heavy-ion fusion reactions. However, the physical correct reasons for description of the large discrepancies in the values of diffuseness parameter are still not clarified. Ghodsi *et al* [21] analyzed the effects of the nuclear incompressibility on the surface diffuseness parameter of the WS potential in the fusion reactions of ^{12}C, ^{16}O, ^{28}Si, and ^{35}Cl projectiles with ^{92}Zr target. The authors applied M3Y-type nucleon–nucleon (NN) forces with an additional repulsive interaction to calculate the inter-nuclear potential. It is shown that the correction effects caused by the saturation property of nuclear matter lead to an increased value of the diffuseness parameter a of about 0.73 fm. This means that the incompressibility of the cold nuclear matter could be responsible for the abnormally large diffuseness of the interaction potential in the fusion process. In another attempt, the authors of [22] employed the classical dissipative trajectory model with the surface friction to make some possible dynamical solutions for describing the abnormally large diffuseness of the WS potential. The next possible interpretation of the anomaly in the diffuseness parameter could be due to an energy-dependent form of the interaction potential, which has been correctly considered to describe the dynamical effects during the fusion reaction [23]. The results of that investigation show that the diffuseness parameter has a decreasing trend with bombarding energy. In [24], the influence of the dynamical effects such as nucleon transfer and dynamical deformation has been studied in connection with diffuseness anomaly within the framework of the improved quantum molecular dynamic model (ImQMD). The diffuseness parameters of the WS potential have been derived for the fusion reactions ^{12}C + ^{92}Zr, ^{16}O + ^{92}Zr, ^{28}Si + ^{92}Zr, ^{35}Cl + ^{92}Zr, ^{40}Ca + ^{46}Ti, and ^{16}O + ^{154}Sm using the dynamical inter-nuclear potential based on the ImQMD simulations. One can find that the obtained values of the diffuseness parameter located in a range between $a = 0.83$ fm and 1.17 fm. Recently, the authors of [25] indicated that the imposing of the thermal considerations of the ion–ion potential plays an important role in increasing the values of the surface diffuseness parameter in heavy-ion fusion reactions. The obtained results confirm that the extracted values of the diffuseness parameter of the WS range from $a = 0.63$ fm to $a = 1.09$ fm.

The study of static and thermal properties of the hot and cold nuclear matter such as nuclear incompressibility, free energy and entropy has always been one of the interesting subjects of nuclear physics and astrophysics especially in the last few years [26–29]. From the physical point of view, one can use the nuclear equation of state (EOS) in order to describe the different properties of NM. For example, the EOS predicted by the density-dependent Seyler–Blanchard (SB) potential is one of the simple and useful approaches to simulate the polarization effects of hot nuclear matter (PEHNM). It is remarkable that the polarized nuclear matter (PNM) is a combination of spin-up (spin-down) protons $P\uparrow(P\downarrow)$ and spin-up (spin-down) neutrons $N\uparrow(N\downarrow)$ so that its total number of nucleons can be determined using the following definition

$$A = P\uparrow + P\downarrow + N\uparrow + N\downarrow\,. \tag{2}$$

The corresponding total density $\rho = \rho_n + \rho_p$ can be written as

$$\rho = \rho_{p\uparrow} + \rho_{p\downarrow} + \rho_{n\uparrow} + \rho_{n\downarrow}. \tag{3}$$

One can indicate for a heavy-ion fusion reaction that the imposing of the PEHNM affetcs the interacting potential between the projectile and the target in the nuclear overlap region where the concept of a two-body potential loses validity. In this situation, it can be therefore interesting and necessary to investigate the polarization effects of hot nuclear matter on the fusion interactions and attempt to see whether these effects can be considered as a correct physical reason for the diffuseness anomaly in heavy-ion fusion reactions. To reach this purpose, the calculations of nucleus–nucleus potential for the selected fusion systems have been carried out using the DF model based on the Paris parametrization of the CDM3Y6-type interaction. We supplement this model with a short-ranged repulsive potential that takes into account the saturation of the nuclear matter. We then impose the PEHNM on the calculations of the nuclear potential using the modified density-dependent SB approach in the T^2 approximation where T is the temperature of the compound nucleus (CN). The values of the surface diffuseness of the nucleus–nucleus potential can be extracted by fitting a WS potential to the original and modified forms of the M3Y-DF potential in the region of the fusion barrier radii. In addition, it should be noted that the thermal effects of CN is applied by assuming it can be considered as a finite piece of hot nuclear matter. In order to examin the validity of the present theoretical approach, we perform a comparison between the calculated and measured fusion cross sections within the framework of the coupled-channels (CC) method for all the colliding systems of interest. We note that these calculations were performed in the so-called isocentrifugal or rotating frame approximation, including couplings to the low-lying 2^+ and 3^- states in both projectile and target.

In section 2 we outline the DF model that is employed to calculate ion–ion potential and the repulsive core potential as well as the EOS of HPNM. Section 3 contains the results and discussion. Section 4 is devoted to some concluding remarks.

2. Theoretical method

Within the framework of the microscopic DF model, one can calculate the ion–ion interaction potential using the following definition

$$V_{\mathrm{DF}}(\boldsymbol{r}) = \int \mathrm{d}\boldsymbol{r}_1 \int \mathrm{d}\boldsymbol{r}_2\, \rho_1(\boldsymbol{r}_1)\rho_2(\boldsymbol{r}_2)\upsilon_{NN}(\boldsymbol{r}_{12} = \boldsymbol{r} + \boldsymbol{r}_2 - \boldsymbol{r}_1). \tag{4}$$

For the evaluation of the strength υ_{NN} of the NN interaction, we use the density-dependent M3Y effective interactions of the Paris-CDM3Y6 type [30]. For the parametrization of the density distributions $\rho_i(\boldsymbol{r})$ of the participant nuclei we employ a two-parameter Fermi–Dirac (2PF) distribution function completed by Hartree–Fock-Bogoliubov (HFB) calculations [31],

$$\rho_i^{\mathrm{2PF}}(r) = \frac{\rho_0}{1 + \exp\left(\frac{r - R_{0i}}{a}\right)}. \tag{5}$$

The values of the average radius R_{0i} and the surface diffuseness a of NM distribution can be taken from HFB calculations [32]. As a result of the literature, several authors pointed out that the original M3Y parametrization for the nucleon–nucleon (NN) interactions predicts correctly the ion–ion potential only for peripheral collisions. In fact, it is shown that the microscopic M3Y-DF potential cannot obtain a satisfactory description of the extreme sub-barrier energies. This fact confirms the existence of a shallow pocket of the potential in the inner part of the fusion barrier. To cure this deficiency, one needs to supplement the calculations of this theoretical model with an effective contact interaction as $\upsilon_{\mathrm{rep}}(\boldsymbol{r}_{12}) = V_{\mathrm{rep}}\delta(\boldsymbol{r}_{12})$ that takes into account the saturation effects of cold NM. According to the recipe proposed in [33, 34], the repulsive potential is proportional to the overlapping volume of the reacting nuclei as follows

$$V_{\mathrm{rep}}(\boldsymbol{R}) = V_{\mathrm{rep}} \int \mathrm{d}\boldsymbol{r}_1 \int \mathrm{d}\boldsymbol{r}_2\, \rho_1(\boldsymbol{r}_1)\delta(\boldsymbol{r}_{12})\rho_2(\boldsymbol{r}_2), \tag{6}$$

where V_{rep} denotes the strength of the repulsive interaction. It is remarkable that the diffuseness of density distributions used in calculating the repulsive part of the potential is characterized by the a_{rep} parameter. In order to access the values of the parameter a_{rep}, we consider the agreement between the theoretical and experimental fusion cross sections. In fact, this parameter at each incident energy is adjusted for a given value of the strength of the repulsive term V_{rep} so that the best agreement with the experimental cross sections is achieved.

2.1. EOS of hot polarized nuclear matter

Polarized nuclear matter is composed of number $P\uparrow(P\downarrow)$ of spin-up (spin-down) protons and $N\uparrow(N\downarrow)$ spin-up (spin-down) neutrons. Under these conditions, the total number A of particles is given by

$$A = P\uparrow + P\downarrow + N\uparrow + N\downarrow. \tag{7}$$

The corresponding densities are $\rho_{p\uparrow}$, $\rho_{p\downarrow}$, $\rho_{n\uparrow}$, and $\rho_{n\downarrow}$. Thus, the total density $\rho = \rho_p + \rho_n$ can be written as

$$\rho = \rho_{p\uparrow} + \rho_{p\downarrow} + \rho_{n\uparrow} + \rho_{n\downarrow}. \tag{8}$$

The three parameters X (neutron excess parameter), Y (spin-up nucleon excess parameter), and Z (spin-up neutron excess parameter) are defined for PNM as follows

$$X = \frac{N\uparrow + N\downarrow - P\uparrow - P\downarrow}{A}, \tag{9}$$

$$Y = \frac{N\uparrow - N\downarrow + P\uparrow - P\downarrow}{A}, \tag{10}$$

$$Z = \frac{N\uparrow - N\downarrow - P\uparrow + P\downarrow}{A}, \tag{11}$$

where the Y and Z parameters are measurements of the asymmetric and polarization specifications of the HPNM. While, parameter X can be actually defined as $X = (N - Z)/(N + Z)$ where N and Z are the total number of the neutrons and protons, respectively. Therefore, one can find that this parameter is only responsible for the asymmetric effects of the nucleons in hot nuclei. Within the framework of the SB approach, the energy per particle of HPNM at finite temperature T can be written in a simple form [35]

$$E(\rho, T) = E_0(\rho, T = 0) + E_T(\rho, T), \tag{12}$$

here $E_0(\rho, T = 0)$ is the total energy per nucleon of HPNM evaluated at $T = 0$ [36]. It can be defined as

$$E = E_V + X^2E_X + Y^2E_Y + Z^2E_Z, \tag{13}$$

where E_V, E_X, E_Y and E_Z are, respectively, the volume, symmetry, spin symmetry, and spin-isospin symmetry energies. These energies are given by

$$E_V = \frac{3\hbar^2C^{2/3}}{10m}\rho^{2/3} + \left(-\frac{a^3C}{3\pi}\rho + \alpha\frac{a^32^nC}{3\pi}\rho^{n+1} + \frac{2a^3C^{5/3}}{5\pi b^2}\rho^{5/3} - \beta\frac{2a^3C^{2/3}}{5\pi}\rho^{2/3}\right)C_1, \tag{14}$$

and

$$E_i = \frac{\hbar^2C^{2/3}}{6m}\rho^{2/3} - \frac{a^3C}{3\pi}\rho C_{i1} + \alpha\frac{a^32^nC}{3\pi}\rho^{n+1}C_{i1} + \frac{4a^3C^{5/3}}{9\pi b^2}\rho^{5/3}C_{i2} - \beta\frac{2a^3C^{2/3}}{9\pi}\rho^{2/3}C_{i3}, \tag{15}$$

where $i = X$, Y, and Z and $C = 3\pi^2/2$. Here, m is the nucleon mass. The values of a, b, α, β, n, C_1, C_{i1}, C_{i2}, C_{i3} based on the modified Seyler–Blanchard potential are tabulated in table 1.

Table 1. Parameters of the modified Seyler–Blanchard potential, equations (14) and (15), which have been used in calculating the volume, symmetry, spin symmetry, and spin-isospin symmetry energies [35, 37]. The corresponding value of the incompressibility constant is $K = 214.3$ MeV.

$a = 0.565$ fm	$b = 9.678$ fm^{-1}	$\alpha = 0.956$
$\beta = 0$	$n = 1/3$	$C_1 = 2393.1$
$C_{X1} = -1357.1$	$C_{X2} = -839.1$	$C_{X3} = -3232.2$
$C_{Y1} = -1211.9$	$C_{Y2} = -621.3$	$C_{Y3} = -3014.4$
$C_{Z1} = -1515.7$	$C_{Z2} = -1077$	$C_{Z3} = -3470.1$

Table 2. The calculated values of the neutron excess parameter X, spin-up nucleon excess parameter Y, and spin-up neutron excess parameter Z for the selected fusion systems. The valence-neutron and -proton orbits as well as the corresponding spin-parity J^{π} of the compound nucleus formed in each reaction are also tabulated using the nuclear shell-model.

Fusion reaction	J^{π}	valence N-orbit	valence Z-orbit	X	Y	Z
^{18}O+^{24}Mg →^{42}Ca	0^+	$f_{7/2}$	$d_{3/2}$	0.04	0.04	0.04
^{16}O+^{26}Mg →^{42}Ca	0^+	$f_{7/2}$	$d_{3/2}$	0.04	0.04	0.04
^{24}Mg+^{30}Si →^{54}Fe	0^+	$f_{7/2}$	$f_{7/2}$	0.03	0.03	-0.03
^{28}Si+^{30}Si →^{58}Ni	0^+	$p_{3/2}$	$f_{7/2}$	0.03	0.03	0.03
^{35}Cl+^{24}Mg →^{59}Cu	$3/2^+$	$p_{3/2}$	$p_{3/2}$	0.01	0.05	0.01
^{16}O+^{63}Cu →^{79}Rb	$5/2^-$	$g_{9/2}$	$f_{5/2}$	0.06	0.03	0.01
^{27}Al+^{45}Sc →^{72}Se	0^+	$f_{5/2}$	$f_{5/2}$	0.05	0.02	-0.02
^{18}O+^{92}Mo →^{110}Sn	0^+	$d_{5/2}$	$g_{9/2}$	0.09	0.01	-0.01
^{28}Si+^{58}Ni →^{86}Mo	0^+	$g_{9/2}$	$g_{9/2}$	0.02	0.06	0.02
^{27}Al+^{70}Ge →^{97}Rh	$9/2^+$	$g_{7/2}$	$g_{9/2}$	0.07	0.07	-0.03
^{27}Al+^{72}Ge →^{99}Rh	$9/2^+$	$g_{7/2}$	$g_{9/2}$	0.09	0.09	-0.01
^{18}O+^{192}Os →^{210}Po	0^+	$g_{9/2}$	$h_{9/2}$	0.20	0.03	0.009

In order to calculate the temperature-dependent part of the energy per nucleon $E_T(\rho, T)$ in the T^2 approximation in equation (12), one can use from the following definition [37]

$$E_T(\rho, T) = -\frac{T^2}{6}\left(\frac{2m^*}{\hbar^2}\right)\left(\frac{3\pi^2}{2}\right)^{1/3}\rho^{-2/3}, \tag{16}$$

where m^* is the nucleon effective mass and is given by

$$m^* = m\left[1 + \frac{m}{\hbar^2}\left(\frac{4a^3ck_f^3}{3\pi b^2}\right)\right]^{-1}, \tag{17}$$

where m is the nucleon mass and k_f is the Fermi momentum. We refer the reader to [37] where the detailed method of computation is described. In order to calculate the temperature values T of the CN related to its excitation energy $E^*_{\rm CN}$, one can use the following relation [38, 39]

$$E^*_{\rm CN} = Q_{\rm in} + E_{\rm c.m.} = \frac{1}{9}AT^2 - T, \tag{18}$$

where A and $Q_{\rm in}$ are the mass number and entrance (incoming) channel Q-value.

2.2. Estimation of the repulsive core parameters

The well-known result of sudden approximation is that when two nuclei overlap each other, the NM density increases in the overlapping region up to $\rho = 2\rho_0$. As a direct consequence of the definition of EOS, the increase of the density in the overlapping region leads to an increase ΔU in the energy of the nucleons of compound (fused) system. By considering the thermal dependence of the CN, the increasing energy of the system can be calculated by [28, 29]

$$\Delta U(T) \approx 2A_P[E(\rho \simeq 2\rho_o, T) - E(\rho \simeq \rho_o, T = 0)], \tag{19}$$

where A_P is the mass number of the projectile nucleus. The EOS introduced by Myers and Swiatecki [36] can be used to estimate the total energy per particle $E(\rho, T = 0)$ of cold nuclear matter. In addition, the energy $E(\rho, T)$ is obtained from equation (12). From the theoretical point of view, one can use the following condition in order to estimate the strength $V_{\rm rep}$ of the repulsive interaction in the complete overlapping region of density distributions [33, 34]

$$V_N(R = 0) = [V_{\rm atr}(R) + V_{\rm rep}(R)]_{R=0} = \Delta U(T), \tag{20}$$

where $V_{\rm atr}(R)$ and $V_{\rm rep}(R)$ can be calculated from equations (4) and (6), respectively.

3. Results and discussion

The aim of this work is to systematically investigate the role of polarization effects of hot nuclear matter on the surface diffuseness of nuclear potential from heavy-ion fusion reactions. We perform calculations for 12 colliding systems involving symmetric ($N = Z$) and asymmetric ($N \neq Z$) nuclei with $96 \leqslant Z_P Z_T \leqslant 608$. The two possible spin orientations of nucleons can be responsible for the polarization effects of hot nuclear matter. However, the spin value of a real nucleus is not simply determined. In the ground-state case, an even–even nucleus has zero spin, while the spins of other nuclei are determined by the odd nucleons which occupy single-particle orbitals. In the present work, the values of X, Y, and Z parameters are calculated based on the nuclear shell-model for all the compound nuclei of interest. The main feature of this model is similar to the atomic shell model except that the conventional WS parametrization accompanied by the spin–orbit potential $V_{\rm so}(r)\ell.s$ was used for the shell-model potential. In addition, we note that the nuclear shell-model utilizes the Pauli exclusion principle to model the structure of atomic nuclei in terms of the energy level. In table 2, we list the values of X, Y, and Z parameters using the nuclear shell-model for the compound nuclei formed in different colliding systems. In this table, the valence-neutron and -proton orbits as well as the corresponding spin-parity J^{π} of these nuclei have been tabulated. In the first step, we calculate the interaction potentials using the microscopic M3Y-DF model for the presently studied fusion reactions. While the ion–ion potential is quite accurately obtained by this model at large separation distances outside the Coulomb barrier, it is unrealistic at short distances between the two interacting nuclei. Because the

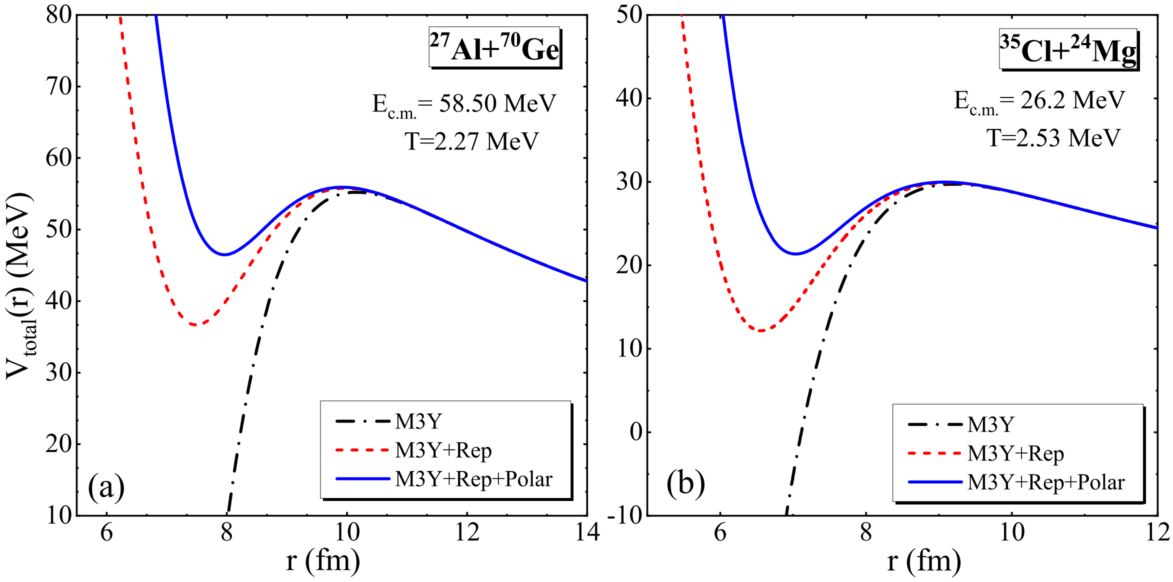

Figure 1. The distribution of total interaction potential versus the separation distance r for (a) ^{27}Al+ ^{70}Ge, and (b) ^{35}Cl+ ^{24}Mg fusion systems using the ordinary M3Y−DF (dash−dotted line), M3Y+Rep (short−dashed line) and M3Y+Rep+Polar (solid line) potential models. In each panel, the values of temperature T (equivalently the incident energy $E_{\rm c.m.}$) have also been presented.

M3Y double-folding potential produces a pocket in the entrance channel potential that is far too deep, even much deeper than the ground-state energy of the compound nucleus. This result can be confirmed by analyzing the distribution of the total interaction potential $V_{\rm tot}(r)$ (in MeV) versus the inter-nuclear distance r (in fm), which is shown in figure 1 for two arbitrary colliding systems ^{35}Cl+ ^{24}Mg at incident energy $E_{\rm c.m.}$=26.20 MeV (equivalently T = 2.53 MeV) and ^{27}Al+ ^{70}Ge at incident energy $E_{\rm c.m.}$= 58.50 MeV (equivalently T = 2.27 MeV). Using the procedure proposed in the previous section, we then simulate theoretically a repulsive core in the NN interactions that reproduces the nuclear matter incompressibility for strong overlap. It should be noted that the results of the modified form of the DF model along with the repulsive core effects are marked as 'M3Y+Rep'. It should be noted that we consider only the volume and symmetry energies, namely E_V and E_X terms in equation (13), for calculations of the M3Y+Rep potentials. As shown in the figure, the extra repulsive force in the effective M3Y nucleon–nucleon interactions mainly affects the shape of interaction potential in the inner regions of the Coulomb barrier. In fact, it causes the appearance of a shallow pocket in the classically allowed region for overlapping configurations. Moreover, it is evident that the introduction of a repulsive potential leads to a larger barrier thickness and thus to a reduction in the fusion cross section. In the next step, we apply the polarization effects of nuclear matter in the studied reactions within the framework of the modified density-dependent SB approach. In this study, the results of the M3Y-DF model accompanied with the 'repulsive core + spin-polarization' effects are labeled as 'M3Y+Rep+Polar'. Here, we consider all terms of E_V, E_X, E_Y, and E_Z in the calculations of the total energy per nucleon of HPNM, equation (13). One can see from figure 1 that the PEHNM mainly affects the shape of interaction potential in the inner regions of the

Table 3. The values of the fusion barrier characteristics and the minimum energy of the pocket obtained from the M3Y double-folding potential and its modified forms for the fusion of ^{35}Cl+ ^{24}Mg and ^{27}Al+ ^{70}Ge.

Reaction	Potential model	R_B (fm)	V_B (MeV)	$V_{\rm pocket}$ (MeV)
^{35}Cl+ ^{24}Mg	M3Y	9.21	29.71	—
	M3Y+Rep	9.12	29.90	12.16
	M3Y+Rep+Polar	9.08	29.96	21.35
^{27}Al+ ^{70}Ge	M3Y	10.15	55.21	—
	M3Y+Rep	9.98	55.76	36.67
	M3Y+Rep+Polar	9.92	55.91	46.48

Coulomb barrier. In reality, these effects lead to the higher Coulomb barriers and much shallower pockets in the inner part of the entrance potential than one predicted by the M3Y +Rep model. In table 3 we list the calculated values of the fusion barrier characteristics ($R_{\rm B}$, $V_{\rm B}$) and the pocket energy ($V_{\rm pocket}$) using the potentials employed in the present work for the fusion of ^{35}Cl+ ^{24}Mg and ^{27}Al+ ^{70}Ge.

Here and in the following we are interested in analyzing the energy-dependent behavior of the fusion cross sections $\sigma_{\rm fus}$ for different colliding systems based on the original and modified forms of the M3Y-DF potential. The theoretical values of the fusion cross section at each incident energy are calculated using the CC approach in the computer code CCFULL [40]. We note that the CC calculations of fusion reactions can be simplified by adopting the rotating frame approximation which allows a drastic reduction of the number of channels used in the calculations. Moreover, it is assumed that the orbital angular momentum is conserved for the relative motion of the dinuclear system. The CC model is based on the close connection existing between the low-lying

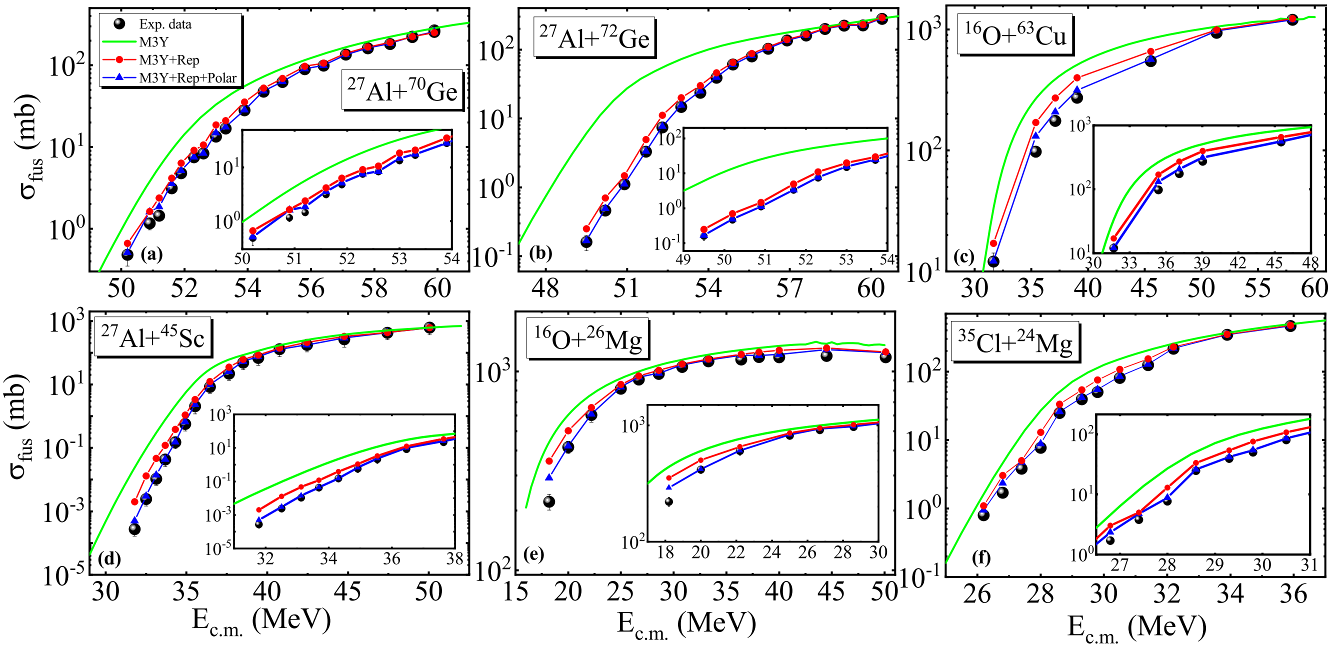

Figure 2. Comparison between the experimental and theoretical values of the fusion cross sections using the CC calculations based on the M3Y, M3Y+Rep, and M3Y+Rep+Polar potentials for fusion systems (a) ^{27}Al+^{70}Ge, (b) ^{27}Al+^{72}Ge, (c) ^{16}O+^{63}Cu, (d) ^{27}Al+^{45}Sc, (e) ^{16}O+^{26}Mg, (f) ^{35}Cl+^{24}Mg.

collective excitations of the reacting nuclei and the near- and sub-barrier heavy-ion fusion cross sections. The result of coupling to such excitations is the distribution of the fusion barrier. One-phonon quadrupole and octupole transitions to low-lying states in projectile and target are included in the calculations. The nuclear structure inputs of the low-lying 2^+ and 3^- states for the systems of interest are taken from [41, 42]. In figure 2, the experimental fusion cross sections are compared with the results of the original and modified forms of the M3Y-DF potential as a function of the center-of-mass energy $E_{c.m.}$ for six colliding systems ^{32}S+^{40}Ca, ^{28}Si+^{28}Si, ^{24}Mg+^{30}Si, ^{18}O+^{74}Ge, ^{27}Al+^{70}Ge and ^{27}Al+^{72}Ge, for example. It is seen that the CC calculations based on the ordinary M3Y potential overestimate the experimental data at whole energy range, in particular at low and near-barrier energies. The results shown in figure 2 reveal that the application of the M3Y+Rep potential seems to help the suppression of the calculated fusion cross sections. This is not only because the potential attains a higher-lying minimum but also because the repulsive effects from the incompressibility of nuclear matter produce a thicker classically forbidden region. A much better agreement between present data and CC calculations over the whole energy range is found when we consider the polarization effects in calculating the total interaction potentials and thus the fusion cross sections. This result is reasonable. Because according to figure 1 the M3Y+Rep+Polar potential lead to a shallower pocket as compared to the results of the M3Y+Rep potential. It is remarkable that the calculations of the fusion excitation functions based on the both M3Y+Rep and M3Y+Rep+Polar potential models have been performed for different bombarding energies of the considered fusion systems.

There is considerable interest in performing research on the role of the polarization effects of HNM on the surface diffuseness anomaly in heavy-ion fusion reactions. In order to realize this goal, we extract the corresponding diffuseness parameters of the WS potential based on the energy-dependent interaction potentials of M3Y+Rep and M3Y+Rep+Polar. For comparison, the values of the parameter a are also determined by fitting the pure M3Y potentials with a WS form in the region of the fusion barrier radii. The detailed results are shown in figures 3 and 4. In these figures, we display the variations trend of the extracted diffuseness parameters as a function of the center-of-mass energy $E_{c.m.}$ for all considered fusion reactions. Our investigations demonstrate clearly that fitting to the WS potential based on the M3Y-DF potentials gives an average value of about 0.61 fm for the diffuseness parameter. This is similar in magnitude to $a = 0.63$ fm of scattering studies [14, 15, 43]. For further understanding, we perform the calculations of the interaction potential using the Skyrme force SkM* with incompressibility $K = 216.7$ MeV. It is well known that the SkM* parameterization is very successful for describing the bulk properties and surface properties of nuclei [44]. The average value of the diffuseness parameter from the Skyrme potentials is $a \approx 0.64$ fm for the selected systems, which is comparable to the values deduced from elastic scattering data. We find that the obtained values of the diffuseness parameter from the M3Y+Rep potentials locate in the range of $a = 0.60$ to 0.77 fm for different colliding systems. This result reveals the importance of the simulation of the nuclear matter incompressibility in the tail region of the nucleus–nucleus potential in heavy-ion fusion reactions. Our findings confirm the effect of incompressibility on the surface diffuseness parameter of the WS potential in heavy-ion fusion reactions [21]. From

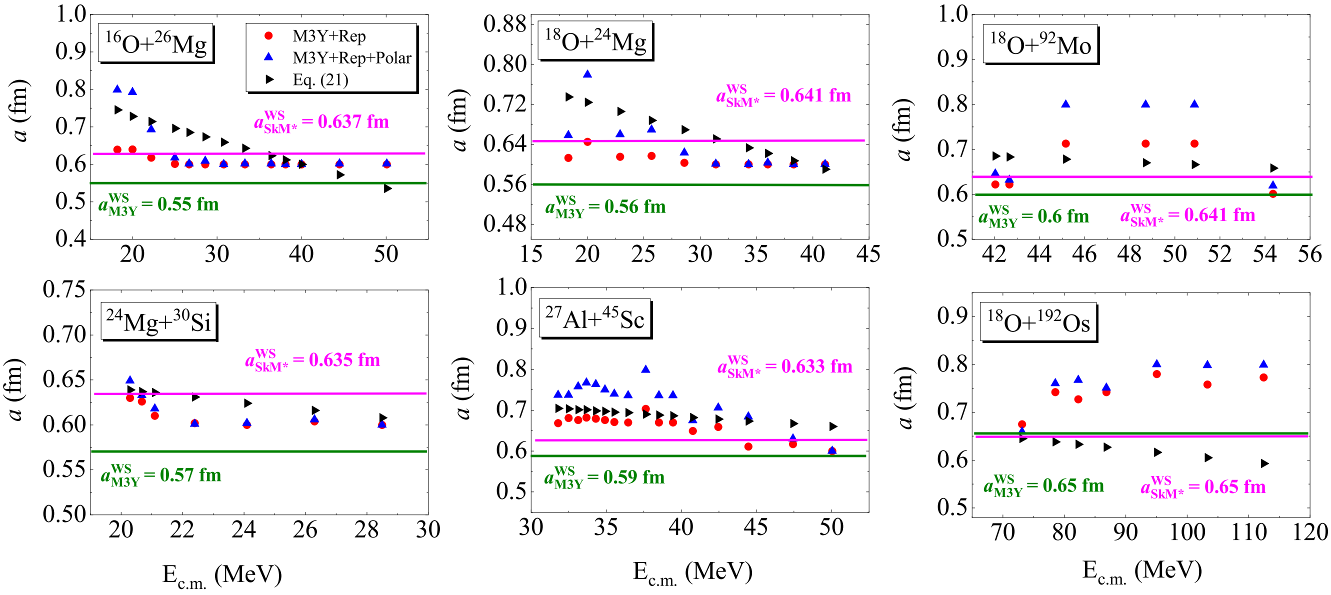

Figure 3. The extracted diffuseness parameter in WS potential as a function of center-of-mass energy based on the M3Y, M3Y+Rep and M3Y+rep+polar potentials for fusion systems (a) ^{16}O+^{24}Mg, (b) ^{18}O+^{24}Mg, (c) ^{18}O+^{92}Mo, (d) ^{24}Mg+^{30}Si, (e) ^{27}Al+^{45}Sc, (f) ^{18}O+^{192}Os. The values obtained by the SkM* parameterization and also equation (21), see text for details, are also shown.

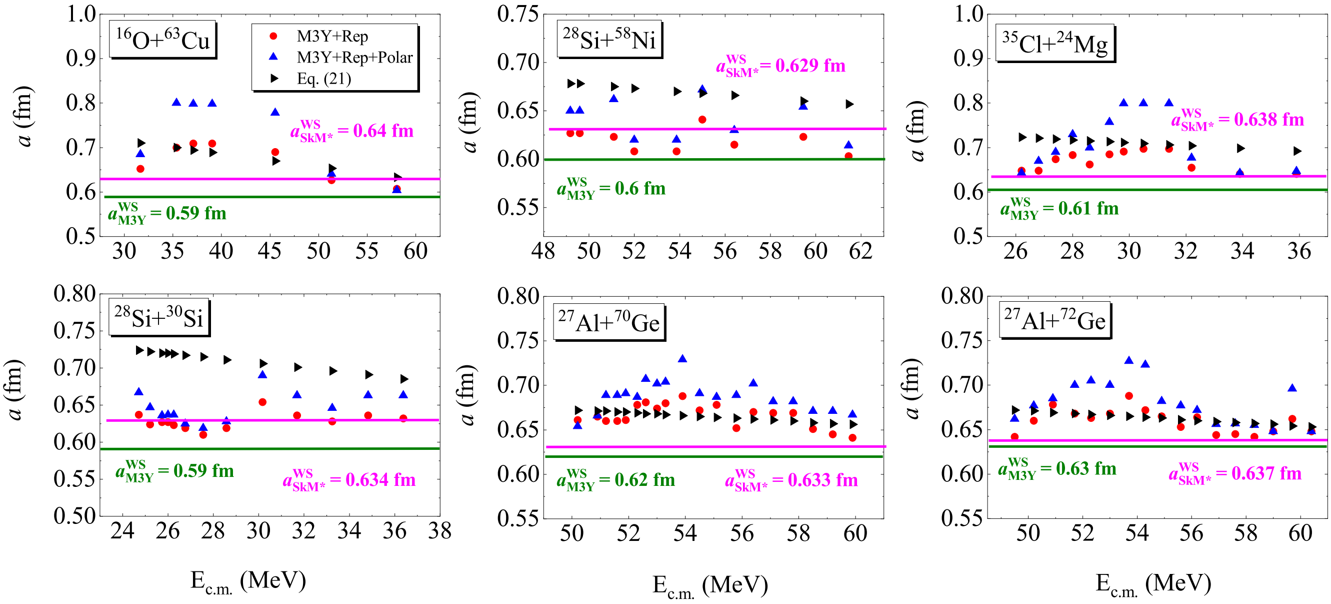

Figure 4. Same as figure 3, but for fusion systems (a) ^{16}O+^{63}Cu, (b) ^{28}Si+^{58}Ni, (c) ^{35}Cl+^{24}Mg, (d) ^{28}Si+^{30}Si, (e) ^{27}Al+^{70}Ge, and (f) ^{27}Al+^{72}Ge.

figures 3 and 4, one can also see that the extracted diffuseness parameters are sensitive to the polarization effects of HNM especially at low energies. In fact, our findings reveal that the PHHNM leads to an increased range of this parameter from $a = 0.61$ to 0.80 fm. In this situation, one can conclude that the polarization effects can be considered as a physical reason for abnormally large diffuseness parameter of the WS potential in the heavy-ion fusion reactions.

Using the obtained values of diffuseness parameter, we suggest the following energy-dependent parametrization scheme for evaluating the values of this parameter

$$a(E_{\mathrm{c.m.}}) = (A_1^{-1/3} + A_2^{-1/3})^{1/2} \times \left[-0.13029\frac{E_{\mathrm{c.m.}}}{B_z} + 0.99859\right], \tag{21}$$

where $B_z = \frac{Z_1 Z_2}{A_1^{1/3} + A_2^{1/3}}$. Moreover, A_1, A_2, Z_1 and Z_2 are the mass and atomic numbers of the projectile and target nuclei, respectively. This formula can be used as a direct method for calculation the diffuseness parameter of nucleus–nucleus

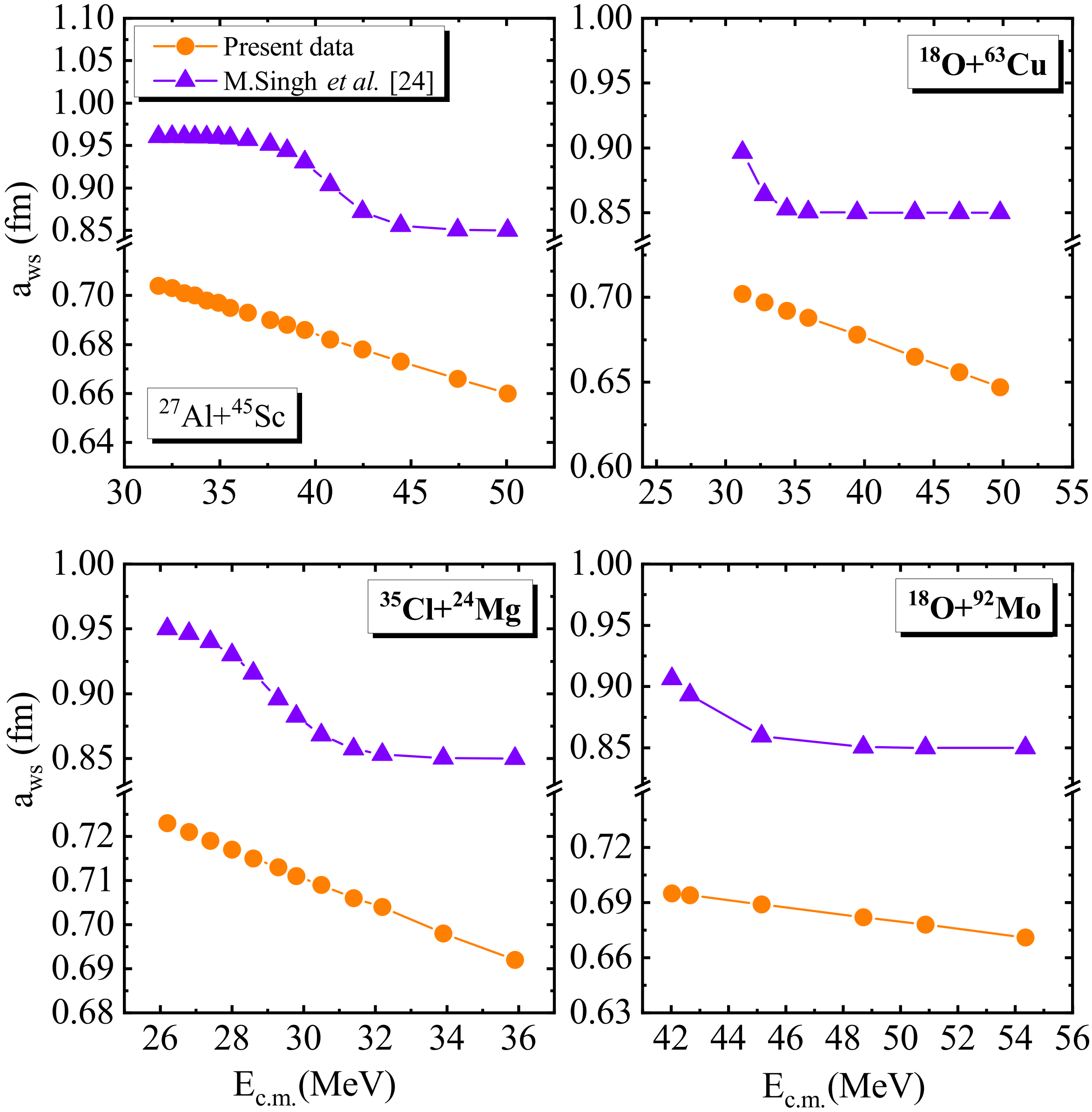

Figure 5. The behavior of the extracted values of the diffuseness parameter on the present equation (green solid circle) as a function of the center-of-mass energy $E_{c.m.}$ for the fusion systems (a) $^{27}Al+^{45}Sc$, (b) $^{18}O+^{63}Cu$, (c) $^{35}Cl+^{24}Mg$, and (d) $^{16}O+^{92}Mo$. The purple solid circles show the results obtined from [23].

potential when the values of (A, Z, and $E_{c.m.}$) quantities are specified for the interaction systems. The values of the diffuseness parameter of WS potential extracted from equation (21) are shown in figure 5 for the fusion reactions $^{27}Al+^{45}Sc$, $^{18}O+^{63}Cu$, $^{35}Cl+^{24}Mg$, and $^{18}O+^{92}Mo$. In this figure, the results of Singh *et al* (purple solid circles) are also shown for comparison. One can see that both models give a decreasing trend for the energy dependence of the diffuseness parameter. Although we find that the sensitivity of the results of Singh *et al* to the changes in the values of the center-of-mass energy $E_{c.m.}$ is more than the present results, especially at low energies. However, the difference between the obtained values of the diffuseness parameter can be attributed to the factors such as the fitting procedure, the selected model for calculating the nucleus–nucleus potential, the intrinsic properties of the selected systems.

4. Conclusions

To summarize, we investigate the role of spin-polarization effects of HNM in interpreting the anomaly in the diffuseness parameter of the WS potential in heavy-ion fusion reactions. Calculations have been performed for 12 colliding systems with the condition $96 \leqslant Z_P Z_T \leqslant 608$ for the charge product of their reacting nuclei. The ion–ion potential is obtained by the double-folding potential with CDM3Y6-Paris effective NN forces supplemented with a repulsive core potential that reproduces the incompressibility of the nuclear matter for total overlap. In order to consider the spin-polarization effects in the calculations of the nuclear potential, we use the EOS predicted by the modified density-dependent Seyler–Blanchard approach. The obtained results show that the role of the spin-polarization effects of HNM in the inner part of the barrier and the depth of the pocket is essential. We conclude that these physical effects of nuclear matter can be responsible for the better agreement between the calculated and measured values of the heavy-ion fusion cross section especially at low energy range. In addition, it was clearly observed that the imposing of the polarization effects of the hot nuclear matter on the nucleus–nucleus potential lead to the increase of the values of the diffuseness parameter of the WS potential. In the present study, the energy dependence of the nuclear potential is included through the energy dependence of the diffuseness parameter of the WS potential. It is observed that the parameter a has a decreasing trend by increasing the center-of-mass energy. The present investigation reveals that the spin-polarization effects of HNM can be considered as a reason for the large discrepancies in diffuseness parameters extracted from scattering and fusion analysis.

References

[1] Negele J W 1982 The mean-field theory of nuclear structure and dynamics *Rev. Mod. Phys.* **54** 913
[2] Umar A S and Oberacker V E 2005 Time-dependent response calculations of nuclear resonances *Phys. Rev.* C **71** 034314
[3] Blocki J, Randrup J, Swiatecki W J and Tsang C F 1977 Proximity forces *Ann. Phys.* **105** 427
[4] Umar A S, Simenel C and Oberacker V E 2014 Energy dependence of potential barriers and its effect on fusion cross sections *Phys. Rev.* C **89** 034611
[5] Bass R 1980 Transport theories of heavy-ion reactions *Prog. Part. Nucl. Phys.* **3** 49
[6] Pardi C I, Stevenson P D and Xu K 2014 Extension of the continuum time-dependent Hartree-Fock method to proton states *Phys. Rev.* E **89** 033312
[7] Royer G and Zbiri K 2002 Asymmetric fission for ^{70,76}Se and ^{90,94,98} Mo via quasimolecular shapes and related formulas *Nucl. Phys.* A **697** 630
[8] Satchler G R and Love W G 1979 Folding model potentials from realistic interactions for heavy-ion scattering *Phys. Rep.* **55** 183
[9] Wang N and Scheid W 2008 Quasi-elastic scattering and fusion with a modified Woods-Saxon potential *Phys. Rev.* C **78** 014607
[10] Newton J O, Butt R D, Dasgupta M, Hinde D J, Gontchar I I, Morton C R and Hagino K 2004 Systematic failure of the Woods-Saxon nuclear potential to describe both fusion and elastic scattering: possible need for a new dynamical approach to fusion *Phys. Rev.* C **70** 024605
[11] Gautam M S 2015 Effects of intrinsic degrees of freedom in enhancement of sub-barrier fusion excitation function data *Mod. Phys. Lett.* A **30** 1550013
[12] Pekeris C L 1934 The rotation-vibration coupling in diatomic molecules *Phys. Rev.* **45** 98
[13] Woods R D and Saxon D S 1954 Diffuse surface optical model for nucleon-nuclei scattering *Phys. Rev.* **95** 577
[14] Silva C P *et al* 2001 The heavy-ion nuclear potential: determination of a systematic behavior at the region of surface interaction distances *Nucl. Phys.* A **679** 287
[15] Christensen P R and Winther A 1976 The evidence of the ion-ion potentials from heavy ion elastic scattering *Phys. Lett.* B **65** 19
[16] Gontchar I I, Hinde D J, Dasgupta M and Newton J O 2003 Surface diffuseness of nuclear potential from heavy-ion fusion reactions *Nucl. Phys.* A **722** 479
[17] Hagino K, Takehi T, Balantekin A B and Takigawa N 2005 Surface diffuseness anomaly in heavy-ion potentials for large-angle quasielastic scattering *Phys. Rev.* C **71** 044612
[18] Leigh J R *et al* 1995 Barrier distributions from the fusion of oxygen ions with ^{144,148,154}Sm and ^{186}W *Phys. Rev.* C **52** 1351
[19] Dasgupta M, Hinde D J, Newton J O and Hagino K 2004 The nuclear potential in heavy-ion fusion *Prog. Theor. Phys. Suppl.* **154** 209
[20] Newton J O, Morton C R, Dasgupta M, Leigh J R, Mein J C, Hinde D J, Timmers H and Hagino K 2001 Experimental barrier distributions for the fusion of ^{12}C, ^{16}O,^{28}Si, and ^{35} Cl with ^{92} Zr and coupled-channels analyses *Phys. Rev.* C **64** 064608
[21] Ghodsi O N and Zanganeh V 2010 The effect of the nuclear state equation on the surface diffuseness parameter of the Woods-Saxon potential in the heavy ion fusion reactions *Phys. Rev.* A **846** 40
[22] Chushnyakova M V and Gontchar I I 2013 Heavy ion fusion: possible dynamical solution of the problem of the abnormally large diffuseness of the nucleus-nucleus potential *Phys. Rev.* C **87** 014614
[23] Singh M, Duhan S S and Kharab R 2011 Diffuseness of Woods-Saxon potential and sub-barrier fusion *Mod. Phys. Lett.* A **26** 2129
[24] Zanganeh V, Gharaei R and Wang N 2017 Dynamical explanation for the anomaly in the diffuseness parameter of the nucleus-nucleus potential in heavy-ion fusion reactions *Phys. Rev.* C **95** 034620
[25] Gharaei R, Hadikhani A and Zanganeh V 2019 An explanation for the anomaly problem of diffuseness parameter of the nucleus-nucleus potential in heavy-ion fusion reactions: a possible thermal solution *nucl. Phys.* A **990** 47
[26] Das C, Sohu R and Tripathi R K 1993 Hot and dense asymmetric nuclear matter *Nucl. Phys.* C **48** 1056
[27] Zhang Y J *et al* 1996 Thermodynamical properties and Coulomb instabilities in hot nuclear systems with the Gogny interaction *Phys. Rev.* C **54** 1137
[28] Ghodsi O N and Gharaei R 2011 Equation of state of hot polarized nuclear matter and heavy-ion fusion reactions *Phys. Rev.* C **84** 024612
[29] Ghodsi O N and Gharaei R 2012 Temperature dependence of the repulsive core potential in heavy-ion fusion reactions *Phys. Rev.* C **85** 064620
[30] Bertsch G, Borysowicz J, McManus H and Love W G 1977 Interactions for inelastic scattering derived from realistic potentials *Nucl. Phys.* A **284** 399
[31] http://www-nds.iaea.org/RIPL-2/masses.html
[32] de Vries H, deJager H and de Vries C 1987 Nuclear charge-density-distribution parameters from elastic electron scattering *At. Data Nucl. Data Tables* **36** 495
[33] Mişicu S ¸ and Esbensen H 2007 Signature of shallow potentials in deep sub-barrier fusion reactions *Phys. Rev.* C **75** 034606
[34] Mişicu Ş and Esbensen H 2006 Hindrance of heavy-ion fusion due to nuclear incompressibility *Phys. Rev. Lett.* **96** 112701
[35] Mansour H M M, Hammad M and Hassan M Y M 1997 Polarized nuclear matter using extended Seyler-Blanchard potentials *Phys. Rev.* C **56** 1418
[36] Myers W D and Swiatecki W J 1998 Nuclear equation of state *Phys. Rev.* C **57** 3020
[37] Mansour H M M and Ramadan K A 1998 Polarized nuclear matter using a modified density dependent Seyler-Blanchard potential *Phys. Rev.* C **57** 1744

[38] Puri R K and Gupta R K 1992 Alpha-cluster transfer process in colliding S-D shell nuclei using the energy density formalism *J. Phys* G **18** 903

[39] Gupta R K, Singh S, Puri R K, Sandulescu A, Greiner W and Scheid W 1992 Influence of the nuclear surface diffuseness on exotic cluster decay half-life times *J. Phys. G: Nucl. Part. Phys.* **18** 1533

[40] Hagino K, Rowley N and Kruppa A T 1999 A program for coupled-channel calculations with all order couplings for heavy-ion fusion reactions *Comput. Phys. Commun.* **123** 143

[41] Raman S, Nestor C W Jr. and Tikkanen P 2001 Transition probability from the ground to the first-excited 2^+ state of even-even nuclides *At. Data Nucl. Data Tables* **78** 1

[42] Kibedi T and Spear R H 2002 Reduced electric-octupole transition probabilities, $B(E3;\, 0_1^+ \rightarrow 3_1^+)$-an update *At. Data Nucl. Data Tables* **80** 35

[43] Chamon L C *et al* 1996 Isotopic dependence of the ion−ion potential in the systems $^{16}O+^{58,60,62,64}Ni$ *Nucl. Phys.* A **597** 253

[44] Bartel J, Quentin P, Brack M, Guet C and Hakansson H B 1982 Towards a better parametrisation of Skyrme−like effective forces: a critical study of the SkM force *Nucl. Phys.* A **386** 79